STOCHASTIC INTEGRATE-AND-FIRE MODEL FOR THE RETINA

Sérgio Capela, Pedro Tomás, Leonel Sousa

INESC-ID / IST TULisbon
Rua Alves Redol 9, 1000-029, Lisboa PORTUGAL
capela@sips.inesc-id.pt, {Pedro.Tomas,Leonel.Sousa}@inesc-id.pt

ABSTRACT

Prostheses are an efficient way of alleviating some of the handicaps suffered by the disabled. One of the most prominent impairments which would greatly benefit from the existence of visual prosthesis is blindness. Several models and training algorithms have been proposed to reach such aim.

This paper presents a stochastic model for the retina and introduces a training method for fitting the model to real data. The model is based on an integrate-and-fire scheme under additive white noise. A gradient ascent training method is used to maximize the probability of occurrence of spike events at a given set of time stamps. The model is trained using real data and the results are evaluated by using different error measures. The quality and the validity of the whole process is discussed based on that analysis.

1. INTRODUCTION

One of the central aspects of neural coding is the relationship between the outside stimuli and the raised neuronal activity inside the brain. In the human visual system, this corresponds to the light intensity projected on the retina and the corresponding sequence of spikes of the excited neurons. However, an important feature of neurons is the variability of elicited responses, even to identical repeats of the same stimuli [1]. For the purpose of modeling such systems, schemes exist that are stochastic in nature and that achieve a proper description of the observed input-output relationship of some sensory responses. One of the most widely used models in this area of neuroscience is the Linear-Nonlinear-Poisson (LNP) model. However this model has a number of shortcomings, one of the most prominent being its low temporal precision. Integrate-and-fire (I&F) models represent a well known alternative for spiking neuron models [2] and constitute a more realistic approach which exhibits a high degree of accuracy [3].

This type of models has been proposed, alongside with parameter estimation techniques [4, 5]. However the type of stimuli used in this paper differs from the ones used in the presented references. Real data is used in this paper, recorded by stimulating a salamander ON cell with a full field white noise visual stimulus, which belongs to a subset of data from [6]. This data was used for testing the model and the proposed maximization method. This work shows that generalized I&F models under additive white noise can be described by a low number of parameters, making use of basis functions to describe the involved filtering processes. Such construction eases the training process by reducing the number of parameter to be fitted. With the purpose of training the model, gradient ascent maximization was implemented based on the probability of the model to reproduce the real responses.

The paper is organized as follows. In section 2 the model for the retina is presented alongside with its mathematical concretization. The stochastic properties of the model are presented and a training method is proposed. Section 3 presents results obtained with real data and evaluates the overall performance of both the model and the training method. Conclusions follow in the last section.

2. THE RETINA MODEL

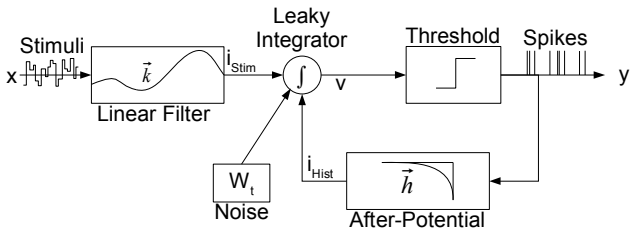

Figure 1: Leaky Integrate-and-Fire Stochastic Model.

The model, depicted in figure 1 has one input, which consists of a visual stimulus, and one output that consists of a sequence of discrete events, usually referred to as spike train. The mechanism responsible for the output is the model's leaky integrate-and-fire (I&F) process, which receives as inputs the convolved visual stimulus i_{Stim}, the convolved output history i_{Hist} and an additive noise source $W_k \sim N(0, \sigma^2)$. Both inputs are described by the following convolutions,

$$i_{Stim_j} = \vec{k} * \vec{x}_j; \quad i_{Hist_j} = \vec{h} * \vec{y}_j. \tag{1}$$

where $\vec{k}$ and $\vec{h}$ are linear filters. The integrand v, known as the subthreshold potential, is described by equation 2:

$$v_j = (1-g)v_{j-1} + i_{Stim} + i_{Hist} + W_j \tag{2}$$

where g denotes the inherent leakage factor of the integrator.

The threshold block of figure 1 is responsible for generating the spike response y of the model, by raising a neural event whenever the integrand surpasses a fixed threshold value V_{th}. When eliciting a spike, the model's subthreshold potential v is reset, hence regenerating the integrative process. This potential is discontinuous due to the threshold block. However, between raised spikes, it follows equation 2 and is thus continuous inside this temporal range which goes by the name of Interspike Interval (ISI). Equation 2, therefore, fully describes the model.

This work was partially supported by FCT under the project POSI/EEA-CPS/61779/2004

The $\vec{k}$ filter was constructed upon a basis set of Laguerre functions as shown in equation 3:

$$\vec{k} = \sum_{i \in N} k_i \cdot \vec{b}_i \tag{3}$$

where k_i are the bases gain coefficients, b_i are the Laguerre bases vectors and N represents the number of used bases. The Z-domain transfer function of the Laguerre bases functions is [7]:

$$h_L[z] = \frac{\sqrt{1-|\varepsilon|}}{1-\varepsilon z} \prod_{i=1}^{k-1} \frac{z-\varepsilon}{1-\varepsilon z} \qquad k = 1, \cdots M \tag{4}$$

where $\varepsilon > 1$ is a constant value which regulates the position of the bases poles and M is the total number of bases used.

The $\vec{h}$ after-potential in equation 1 was chosen to be a negative exponential,

$$\vec{h} = -G_h e^{-\alpha_h t} \tag{5}$$

with a G_h gain and a α_h decaying rate. The decaying rate defines the length of the after-potential and consequently the recent history taken in account by the model.

2.1 Stochastic Properties of the Model

The W_j term in equation 2 represents the noise in the system which is assumed to be white of variance σ^2 and zero mean. As such, the potential v follows a gaussian density function.

Assuming that there is a space of n samples, at the rate of $1/dt$, until the occurrence of the next spike, the model's stochastic nature gets characterized by the following geometric rule,

$$v_n \sim (1 - g \cdot dt) v_{n-1} + W_n, \tag{6}$$

where dt is the sampling period.

Therefore, the i'th sample potential is affected by $W_i \sim N\,(0, \sigma_i^2\,)$ where,

$$\sigma_i^2 = \sigma^2 \sum_{k=0}^{i} \alpha^{2k} = \sigma^2 \frac{1-\alpha^{2(i+1)}}{1-\alpha^2}, \tag{7}$$

and $\alpha = (1 - g \cdot dt)$.

Thus, assuming that W_j is white noise, the potential curve follows a gaussian time series $N(v|\mu_j, \sigma_j^2)$, where the mean is directly taken of the model mathematical formulation (equation 2), for a particular sample time k, and the variance is given by the geometric rule already introduced in equation 7.

The total set of model parameters θ, from which the mean and the variance are extracted is therefore:

$$\theta = \{g, k_1, \cdots, k_N, G_h, \alpha_h, \sigma\} \tag{8}$$

leading to a total of $N+4$ parameters.

2.2 Training the Model

These type of models are referred to as point process models for generating sequences of events. Thus, for all purposes in the current work there is only two known variables: the times of occurrence of the spikes and the visual stimuli. No information whatsoever is given about the subthreshold potential itself, which is seen as a hidden variable. That poses a problem since an initial guess of the parameters has to be made in order to construct the potential curve inside the ISI.

Once this initial guess for the parameters is made, a gradient ascent technique is used to maximize the spike occurrence probability at the observed times.

2.2.1 Assessing the Probabilities of Occurrence

Dividing the time line of the v subthreshold potential in several time bins according to a certain sampling time, the idea is to maximize the probability for the model to fire at the end of the interval and not firing in the preceding time bins. Using Bayes rules on the probability of the ISI $P(\neg S_1, \cdots, \neg S_{n-1}, S_n)$, results in:

$$\begin{aligned} L =& P(\neg S_1, \neg S_2, \cdots, \neg S_{n-1}, S_n) = \\ =& P(\neg S_2, \cdots, \neg S_{n-1}, S_n | \neg S_1) P(\neg S_1) = \\ =& P(\neg S_1) P(\neg S_2 | \neg S_1) P(\neg S_3 | \neg S_2) \cdots P(S_n | \neg S_{n-1}) \end{aligned} \tag{9}$$

where $P(\neg S_i)$ represents the probability of not firing in the i'th time bins and $P(S_n)$ represents the probability of the neuron firing at the n'th time bin. Being the ISIs independent among themselves, these gain functions are extensible in order to contain several ISIs.

To maximize these functions, the application of the natural logarithm function facilitates the computation as it transforms the multiplication in a sum of log probabilities:

$$\begin{aligned} l = \ln L = \ln P(\neg S_1) + \sum_{k=2}^{n-1} \ln P(\neg S_k | \neg S_{k-1}) + \\ + \ln P(S_n | S_{n-1}) \end{aligned} \tag{10}$$

where,

$$P(\neg S_k | \neg S_{k-1}) = \int_{-\infty}^{V_{th}} N(v|\mu_k, \sigma_k^2) dv \tag{11a}$$

$$\begin{aligned} P(S_n | \neg S_{n-1}) &= \int_{V_{th}}^{\infty} N(v|\mu_n, \sigma_n^2) dv \\ &= 1 - P(\neg S_n | \neg S_{n-1}) \end{aligned} \tag{11b}$$

and V_{th} corresponds to the potential threshold of the rectification block. The goal is to achieve the highest probability with a suitable set of parameters and an acceptable noise variance.

In order to apply gradient ascent techniques, thus maximizing the probabilities of spike occurrence at the observed times, the derivatives in order to the parameters are taken:

$$\begin{aligned} \frac{\partial l}{\partial \theta_i} =& \frac{1}{P(\neg S_1)} \frac{\partial}{\partial \theta_i} P(\neg S_1) + \\ &+ \sum_{k=2}^{n-1} \frac{1}{P(\neg S_k | \neg S_{k-1})} \frac{\partial}{\partial \theta_i} P(\neg S_k | \neg S_{k-1}) + \\ &+ \frac{1}{P(S_n | \neg S_{n-1})} \frac{\partial}{\partial \theta_i} P(S_n | \neg S_{n-1}) \end{aligned} \tag{12}$$

Given the Laguerre bases structure of the $\vec{k}$ filter, the derivatives are then taken in respect to each of the individual bases gains $(k_i, i \in 1, 2, 3, \cdots, N)$ for each of the j sample times and according to the limits imposed in equations 11 $(l_1 = -\infty, l_2 = V_{th})$ and $(l_1 = V_{th}, l_2 = \infty)$:

$$\frac{\partial P_j}{\partial k_i} = -\left(\vec{b}_i * \vec{x}_j\right) dt \int_{l_1}^{l_2} N'\left(v|\mu_j(k_i), \sigma_j^2\right) dv \tag{13}$$

where the $(\vec{b}_i * \vec{x}_j)$ term represents the convolution between the i'th basis and the stimulus chunk of interest. The $N'(v|\mu_j, \sigma_j^2)$ represents the derivative of the Gaussian density function in order to the stochastic variable v.

Given the exponential structure of the after-potential and the resultant two tunable parameters, G_h and α_h, the derivatives can be computed as:

$$\frac{\partial P_j}{\partial G_h} = \left(y_j * e^{-\alpha_h \cdot t}\right) dt \int_{l_1}^{l_2} N'\left(v|\mu_j(G_h), \sigma_j^2\right) dv \qquad (14)$$

where $(y_j * e^{-\alpha_h \cdot t})$ is the convolution between the observed spike train and the gainless exponential, and:

$$\frac{\partial P_j}{\partial \alpha_h} = G_h \left(y_j * -t \cdot e^{-\alpha_h \cdot t}\right) dt \int_{l_1}^{l_2} N'\left(v|\mu_j(\alpha_h), \sigma_j^2\right) dv \qquad (15)$$

where $(y_j * t \cdot e^{-\alpha_h \cdot t})$ is the convolution between the observed spike train and the derivative of the gainless exponential in respect to α_h.

At last, taking the derivative in order to the leakage potential:

$$\frac{\partial P_j}{\partial g} = \mu_j'(g) \int_{l_1}^{l_2} N'\left(v|\mu_j(g), \sigma_j^2(g)\right) dv - \\ - \frac{\sigma_j'(g)}{\sigma_j(g)} \left[(v - \mu_j(g)) N\left(v|\mu_j(g), \sigma_j^2(g)\right) \right]_{l_1}^{l_2} \qquad (16)$$

where $[f(v)]_{l_1}^{l_2} = f(v = l_2) - f(v = l_1)$. Taking also the unknown noise standard deviation as adjustable:

$$\frac{\partial P_j}{\partial \sigma} = -\frac{1}{\sigma} \left[(v - \mu_j) N\left(v|\mu_j, \sigma_j^2(\sigma)\right) \right]_{l_1}^{l_2} \qquad (17)$$

Given the above set of equations, the goal is to achieve, through gradient ascent, a set of parameters that match the experimental results with a relatively high probability of the gain function and an affordable variance for the noise source.

2.2.2 Gradient ascent technique

The gradient ascent technique is iterative and described by equation 18:

$$\theta_{n+1} = \theta_n + \gamma_n \nabla(\theta_n), n \geq 0, \qquad (18)$$

where θ represents the adjustable model parameters and γ the step sizes used in this adjustment. The step sizes are variable during the process and calculated according to the adaptive steps rule from [8],

$$\gamma_n = \begin{cases} u\gamma_{n-1} & \text{, if } \nabla(\theta_n)\nabla(\theta_{n-1}) > 0 \\ d\gamma_{n-1} & \text{, if } \nabla(\theta_n)\nabla(\theta_{n-1}) < 0 \end{cases} \qquad (19)$$

where,

$$u = 1 + \delta_u \quad d = 1 - \delta_d \qquad (20)$$

$$\delta_u \approx \delta_d \ll 1 \qquad (21)$$

2.2.3 First Guess

In order to apply the iterative gradient ascent method, one has to guess an initial value of the parameters. This guess must be carefully made, so that the initial parameters lead to a finite probability and provide a good initial point to start the ascent.

For that purpose, the leakage term was set to a physiologically plausible value $(50ms^{-1})$ [5] and the filters weights were computed using least squares linear regression to approximate the spike-triggered average (STA) [9] of the pair stimulus-spikes used for the training. Those initializations are then used to approximate the after-potential parameters under the minimum possible noise variance. It should be noted that the STA is however an unscaled estimation based on white noise analysis, and as such, it cannot be applied under input signals other than white noise signals. An initial scaling of the $\vec{k}$ filter of figure 1was also done by adjusting a common gain G_k to all the basis.

3. EXPERIMENTAL RESULTS

The presented I&F model is a simplified one and has a restricted regime of applicability. It is under a biologically relevant regime that the model must be analyzed. The proposed training method was implemented and tested with the experimental data used in [6]. These data consists of 12 trials of full field white noise stimulation for a salamander ON cell, where each trial has a duration of 10 seconds with an average count of 8.34 spikes per second. Only the first half of the data was effectively used for the training process, being the second half used for testing purposes.

To assess the quality and the validity of the proposed model and respective training procedure, we compare our results with both real data and data generated by a trained Linear-Nonlinear-Poisson (LNP) model. This model was chosen for comparison purposes due to its popularity and simplicity: it consists of a simple linear filter followed by a non-linearity and a Poisson spike generator [10]. In the results presented herein, it was used a $1ms$ sampling period and the $\vec{k}$ filter was set to a length of $500ms$ and constructed upon 10 basis vectors (see equation 3), which were enough to provide a quite good approximation of the STA. The threshold value V_{th} was set to 1 and the reset value was set to zero. It was also assumed an absolute refractoriness period of $1ms$, during which the integrative process is stalled.

The spike train responses of the trained models and the real responses are depicted in figure 2 for the testing portion of the stimulus (last 5s), which was not used in the training process. Looking directly at these spike trains, one can see that most patterns of the response are indeed generated when using the trained stochastic I&F and that the model clearly outperforms the LNP model.

The use of known error measures based on distance metrics and firing rates provide a comparison of the depicted results from a numerical stance. Two spike metrics proposed in [11] were used for a direct comparison of the trained models responses with the real observed responses. These metrics evaluate the cost of transforming one given spike sequence into another. The first of these metrics accounts for the cost associated with the absolute time of occurrence of neuronal events (SpikeTime Metric) and the second one accounts for the cost in changing the ISIs lengths (InterSpike Metric). The

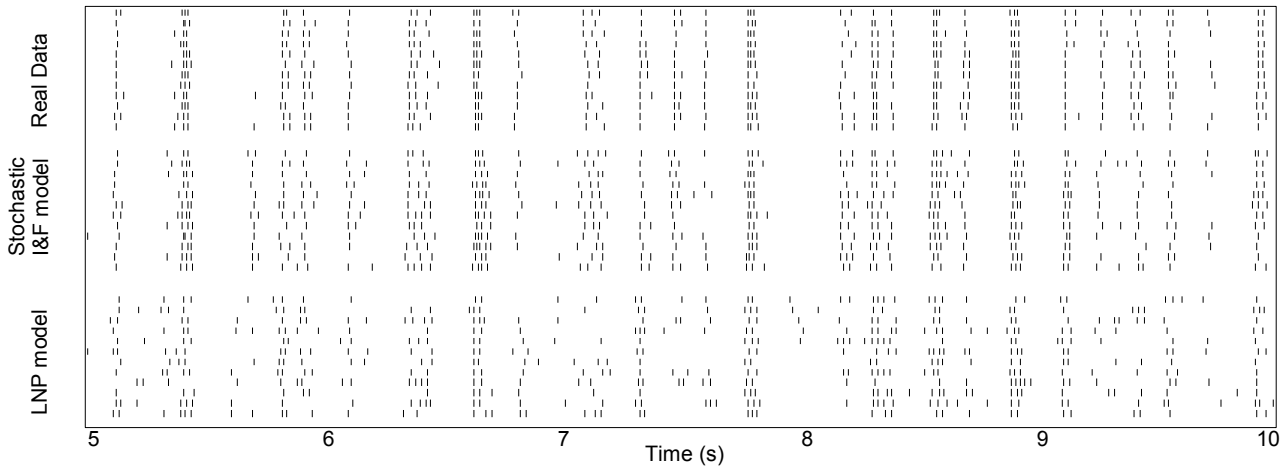

Figure 2: Real and estimated neuronal responses.

results of the metrics applied to both the real responses and the models estimated responses are presented in table 1. The measures in the table are further separated regarding the train portion of the data (the first 5s) and the testing portion (the last 5s). Values in the table's *real vs model* rows are cross-evaluations between the real trials and the estimated trials. The table specific values were calculated using an associated q cost value of $50s^{-1}$ (see [11]). The LNP results were only evaluated for the last 5s of testing data.

Analyzing table 1, one can observe that the results are relatively better (lower) when using the SpikeTime metric. This indicates that one of the model's advantages is its temporal precision, which is better according to the results and in comparison with the LNP model. This result is evident by looking at the spike trains. As expected, cross-comparisons of real and estimated data generally have the highest values. This means that there is a greater difference between spike trains when these are taken from different sets.

A firing rate metric was also used as an auxiliary measure, in which the normalized mean squared error (NMSE) [12] was applied. For that purpose, the firing rates where estimated for both the real and the estimated data, by convolving their PeriStimulus Time Histogram (PSTH) [10] with a Gaussian window of zero mean and $\sigma^2 = 20ms$. The results are once again in table 1 and attest once more the superiority of the I&F model. Figure 3 further illustrates the good behavior of the model by displaying portions of the estimated firing rates. The approximated firing rate of the I&F model is close to the real in both the train an the test portions of the signals and the close values of the NMSE are a good evidence of what is shown in the depicted firing rates.

A third set of results is present in the column "spike count" of table 1 in order to compare the number of spikes observed. From the results it is seen that there is a slight difference in the number of spike occurrences in both the train and the test data, which can be explained with the incapacity of the model to achieve certain patterns of the real responses. Nonetheless, these differences are not expressive and are also present in the LNP model.

Some final remarks should be made. In respect to the after-potential, the training tended to annul the negative exponential by setting its gain to very low values, which could mean that this particular type of after-potential is not suitable for the given real data. It was also observed that the convergence of the standard deviation of the noise source usually leads to relatively high values when compared to the potential threshold used. To alleviate such problem, part of the training was done by forcing the evolution of the standard deviation to lower numerical values.

Table 1: Error measures of the trained models responses and the real responses.

		Spike Time	Inter Spike	Spike Count	NMSE
Training					
Real	mean	21.84	29.06	39.42	
	std	2.47	3.61	2.07	
I&F	mean	30.60	36.20	35.83	
	std	3.35	2.54	2.59	
Real vs I&F	mean	32.27	40.30		0.23
	std	2.83	3.14		
Testing					
Real	mean	20.35	29.63	44.00	
	std	2.37	4.01	2.30	
I&F	mean	31.60	40.73	47.25	
	std	2.71	3.67	2.45	
Real vs I&F	mean	31.62	41.99		0.18
	std	2.84	3.62		
LNP	mean	39.63	42.52	40.58	
	std	3.14	2.53	3.42	
Real vs LNP	mean	38.01	44.50		0.25
	std	3.20	2.27		

mean - mean result std - standard deviation

4. ACKNOWLEDGEMENTS

The experimental data used in this paper was gently provided by Prof. Markus Meister

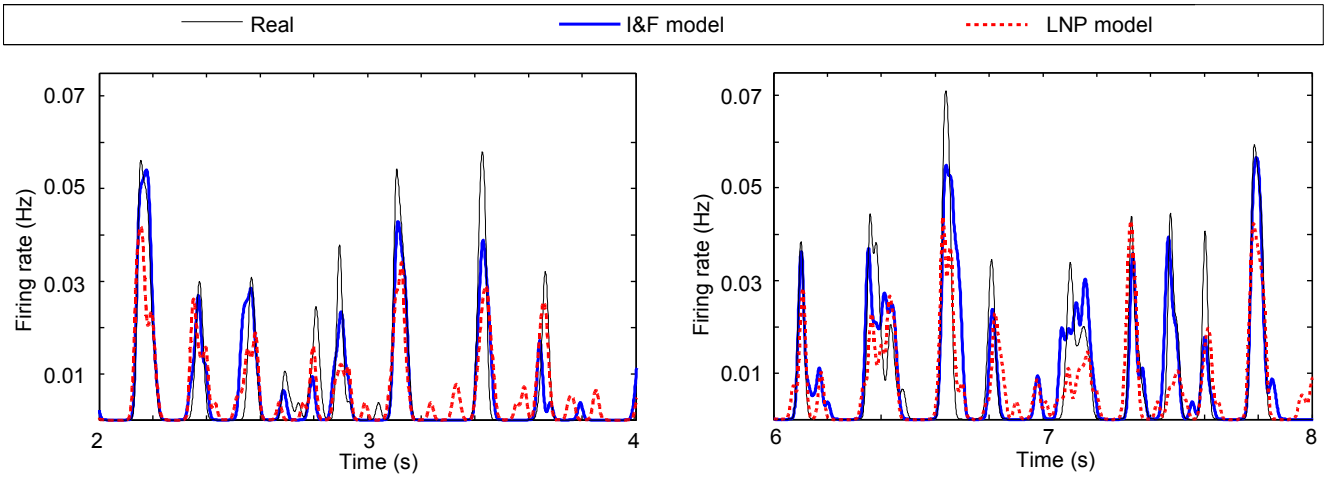

(a) Firing rate graphical comparison for the train set.

(b) Firing rate graphical comparison inside for the testing set.

Figure 3: Comparison between the estimated and observed firing rates.

5. CONCLUSIONS

The work herein shows that the proposed stochastic integrate-and-fire model is indeed capable of exhibiting most of the response patterns seen in real data recorded from cells of the visual system of live specimens. This is achieved with a relatively low number of parameters, in contrast to some of the widely used models in neuroscience. The model is also suitable when high temporal precision is needed, which is one of the strengths of the proposed model.

The model is also, due to their specific mathematical formulation, computationally tractable and as such, the parameters that govern their behavior can be learned. Here, a method based on gradient ascent techniques and on a simple Gaussian based gain function was presented and implemented. It was shown that this method can lead to good results, closely matching real data in numerous response patterns. Nevertheless, it could not match some of them, which means that there is room for improvement. In fact, noticing that the gain of the after-potential tended to zero values, leads to the conclusion that more flexible forms of taking into account the memory of visual neurons could improve the results. A simple change in the after-potential form, for example applying basis functions as in the time filter, could also improve the results as well as the flexibility of the model.

REFERENCES

[1] M. Meister and M. J. B. II, "The neural code of the retina," *Neuron*, vol. 22, pp. 425–450, 1999.

[2] W. Gerstner and W. Kistler, *Spiking Neuron Models: Single Neurons, Populations, Plasticity*. Cambridge University Press, 2002.

[3] R. Jolivet, T. J. Lewis, and W. Gerstner, "Generalized integrate-and-fire models of neuronal activity approximate spike trains of a detailed model to a high dgree of accuracy," *Journal of Neurophysiology*, vol. 92, pp. 959–976, 2004.

[4] J. W. Pillow, L. Paninski, V. J. Uzzell, E. P. Simoncelli, and E. J. Chichilnisky, "Predition and decoding of retinal ganglion cell responses with a probabilistic spiking model," *The journal od Neuroscience*, vol. 25, no. 47, pp. 11 003–11 013, November 2005.

[5] L. Paninski, J. W. Pillow, and E. P. Simoncelli, "Maximum likelihood estimation of a stochastic integrate-and-fire neural encoding model," *Neural Computation*, vol. 16, pp. 2533–2561, 2004.

[6] J. Keat, P. Reinagel, R. C. Reid, and M. Meister, "Predicting every spike: A model for the responses of visual neurons," *Neuron*, vol. 30, pp. 803–817, June 2001.

[7] H. Akçay and B. Ninness, "Orthonormal basis functions for modelling continuous-time systems," *Signal Processing*, vol. 77, no. 1, pp. 261–274, 1999.

[8] L. B. Almeida, T. Langlois, J. D. Amaral, and A. Plakhov, *Parameter Adaptation in Stochastic Optimization*. Cambridge University Press, 1998, ch. 6.

[9] L. Paninski, "The spike-triggered average of the integrate-and-fire cell driven by gaussian white noise," *Neural Computation*, 2006.

[10] E. J. Chichilnisky, "A simple white noise analysis of neuronal light responses," *Network: Computation in Neural Systems*, 2001.

[11] J. D. Victor and K. P. Purpura, "Metric-space analysis of spike trains: theory, algorithms and application," *Computation Neural Systems*, vol. 8, pp. 127–164, 1997.

[12] M. J. B. II and M. Meister, "Refractoriness and neural precision," *The Journal of Neuroscience*, 1998.